Nuclear Science and Techniques (2024) 35:150
https://doi.org/10.1007/s41365-024-01496-0

Design and high-power testing of offline conditioning cavity for CiADS RFQ high-power coupler

Ruo-Xu Wang[1,2] · Yuan He[1] · Long-Bo Shi[1] · Chen-Xing Li[1] · Zong-Heng Xue[1] · Tian-Cai Jiang[1] · Xian-Bo Xu[1] · Lie-Peng Sun[1] · Zhou-Li Zhang[1]

Received: 17 October 2023 / Revised: 10 January 2024 / Accepted: 30 January 2024 / Published online: 29 August 2024

Abstract
To validate the design rationality of the power coupler for the RFQ cavity and minimize cavity contamination, we designed a low-loss offline conditioning cavity and conducted high-power testing. This offline cavity features two coupling ports and two tuners, operating at a frequency of 162.5 MHz with a tuning range of 3.2 MHz. Adjusting the installation angle of the coupling ring and the insertion depth of the tuner helps minimize cavity losses. We performed electromagnetic structural and multiphysics simulations, revealing a minimal theoretical power loss of 4.3 %. However, when the cavity frequency varied by 110 kHz, theoretical power losses increased to 10 %, necessitating constant tuner adjustments during conditioning. Multiphysics simulations indicated that increased cavity temperature did not affect frequency variation. Upon completion of the offline high-power conditioning platform, we measured the transmission performance, revealing a power loss of 6.3 %, exceeding the theoretical calculation. Conditioning utilized efficient automatic range scanning and standing wave resonant methods. To fully condition the power coupler, a 15° phase difference between two standing wave points in the conditioning system was necessary. Notably, the maximum continuous wave power surpassed 20 kW, exceeding the expected target.

Keywords RFQ cavity · Power coupler · Offline conditioning · Resonant cavity

1 Introduction

The Chinese initiative accelerator driven subcritical system (CiADS), currently under development at the Institute of Modern Physics, Chinese Academy of Sciences (IMP, CAS), is a multi-MW proton source for energy generation and long-half-life nuclear waste transmutation [1–3]. This national major science and technology infrastructure adopts the continuous wave (CW) and superconducting technical route, capable of accelerating a 5 mA proton beam to 500 MeV in energy. It comprises an intense-beam driver linac, a high-power spallation target station, and a subcritical-mode nuclear reactor. The driver superconducting radio frequency (SRF) linac accelerates the high-intensity proton beam to high energy, which then bombards a spallation target, producing neutrons with a wide spectrum and high flux capable of driving a chain reaction in a subcritical reactor. This process releases nuclear energy and transmutes long-lived nuclear waste. The linac accelerator's front end features a four-vane radio frequency quadrupole (RFQ) cavity operating at a frequency of 162.5 MHz, with a proton energy at the cavity outlet of 2.1 MeV. Injecting 96 kW of driving radio frequency (RF) power into the RFQ cavity, it spans a length of 4883.8 mm.

In the RFQ cavity design, four couplers share the required driving power and are situated at two different longitudinal positions, with each of the two couplers placed at the same longitudinal position. Each coupler necessitates a nominal RF power of 26 kW for CW operation and a maximum transmitted power of 60 kW. The primary function of the

This work was supported by the Chinese initiative accelerator driven subcritical system and the hundred talents plan of the Chinese Academy of Sciences (No.E129841Y).

✉ Yuan He
hey@impcas.ac.cn

✉ Zhou-Li Zhang
zhangzhouli@impcas.ac.cn

[1] Institute of Modern Physics, Chinese Academy of Sciences, Lanzhou 730000, China

[2] Lanzhou University, Lanzhou 730000, China

power input coupler is to link the RFQ cavity to the power source, which supplies microwave power, while also utilizing a ceramic window to isolate the atmosphere from the ultra-high vacuum environment within the RFQ cavity. Consequently, the ceramic window stands as one of the critical components of the accelerator, determining the long-term stable operation of the RFQ cavity [4, 5]. Several factors contribute to the cracking of the ceramic window. Firstly, the secondary electron multipactor effect around the window can cause it to overheat, leading to damage and ultimately cracking [6–9]. Secondly, improper high-frequency structure of the power input coupler can result in excessive electric field around the window, thus causing RF electrical breakdown. Thirdly, inadequate design of the mechanical structure can lead to overheating of the window, resulting in excessive thermal stress. Moreover, unreasonable mechanical structure design can also cause excessive temperature of the coupling loop, reducing coupling strength and increasing power reflection [10]. Additionally, defects in the processing of the power coupler and the smelting of materials produce dust and metal burrs on the inner surface of the power coupler, leading to cavity contamination. Hence, offline RF conditioning and power tests are necessary before the coupler is connected to the RFQ cavity to verify the structural design's reasonability and reduce cavity contamination from the coupler.

At least two couplers are required for offline high-power tests of the power input couplers, typically connected by either a resonant cavity or coaxial connector [11–18]. The coaxial connector requires inner conductors for connection, making it suitable for electrical coupling, such as with high-power couplers for superconducting cavities. In contrast, the resonant cavity does not necessitate inner conductors for connection and can be used for both electrical and magnetic coupling. Magnetic coupling is employed to supply power to the RFQ cavity, utilizing a coupling loop structure where inner conductors cannot be connected. Consequently, the resonant cavity is commonly utilized for offline RF conditioning and high-power tests. For instance, the RFQ cavity of the European spallation source (ESS) operates at a frequency of 352.1 MHz, with two high-power input couplers utilized to feed 1.6 MW of peak power [19]. During offline tests, a resonant cavity was employed, with each coupler subjected to a target power of 1MV peak power and a duty cycle of 5 %. The S11 and S21 parameters of the test cavity were −27 dB and −0.2 dB, respectively, with a power loss of 4 %. Similarly, the RFQ cavity of the International Fusion Materials Irradiation Facility (IFMIF) operates at a frequency of 175 MHz, with eight high-power input couplers adopted to feed 1.28 MW continuous wave power. To conduct offline tests of these high-power input couplers, the IFMIF project also employed a resonant cavity [20]. The target power for each coupler during tests was 200kW continuous wave power. The S11 and S21 parameters of the test cavity were −29 dB and −0.31 dB, respectively, with a power loss of 7 %.

Based on the preceding discussions, resonant cavities are typically preferred as connections for high-power couplers during offline RF conditioning and power tests, particularly for those high-power input couplers that supply power to the cavity utilizing magnetic coupling. For cavities operating at high frequencies, pill box structures [15–18] or rectangular resonators [11–14] are commonly employed for offline tests of high-power couplers. However, given that the frequency of the CiADS RFQ cavity is 162.5 MHz, using the aforementioned types of cavities would result in larger cavity dimensions and lower transmission efficiency. Hence, this paper proposes a low-loss resonant and compact structure cavity designed specifically for offline tests of high-power input couplers for the CiADS RFQ. The cavity was designed using numerical calculation methods, and subsequent high-power tests were conducted.

2 Design of high-power input coupler structure

This study focuses on the high-power testing of power couplers; therefore, this section briefly describes the structural design of the high-power coupler. The primary function of the high-power coupler is to transfer RF power from the power source to the RFQ cavity [4, 5]. Additionally, it acts as a barrier between the air-side transmission line and the RFQ cavity, maintaining a vacuum. The high-power input coupler should sustain specified power under different operating conditions (continuous wave or pulsed) without degrading cavity performance or beam quality. Hence, during the design phase, efforts must be directed toward the following areas. Firstly, achieving excellent radio frequency transmission performance is essential to reduce RF power loss. Secondly, optimizing the electromagnetic field distribution is desired to minimize RF electric breakdown around the ceramic window. Thirdly, to ensure the long-term stable operation of the power coupler, multipacting should be avoided at nominal power. The RF window maintains a high vacuum and ultra-clean environment inside the cavity, so it is essential to ensure the window's reliability from various perspectives throughout the development process. Therefore, comprehensive safety analysis for the window is required during the design phase, and a comprehensive interlock system should be implemented to monitor all activities during offline conditioning and routine operations. These safety analyses typically include radio frequency performance, thermal-mechanical stress at nominal radio frequency power and pressure, and the design of the cooling channel. Monitors often include vacuum levels, arc discharging, and overheating. Generally, when the processing of a new coupler

structure is completed, offline conditioning is necessary to validate the design rationality of the power coupler.

The general layout of the high-power coupler for the CiADS RFQ cavity is depicted in Fig. 1. It comprises a coupling loop module, coaxial transmission line module (RF window and coaxial line), and impedance match module. Each module is detachable via a flange connection. The inner conductor of the coaxial transmission line module is crafted from oxygen-free copper and cooled by deionized water. The impedance match module is constructed from aluminum.

Due to the high-power input coupler's design power of 60 kW, it is essential to cool both the inner and outer conductors of the ceramic window. The IFMIF RFQ cavity utilized a λ/4-long cooling water port for heat dissipation by the high-power input coupler, with the inlet/outlet of cooling water positioned at the end cooling port. However, this design led to the power coupler occupying excessive space [21]. To ensure a compact structure for the CiADS RFQ cavity's coupler, a T-box structure was adopted for the inner conductor cooling channel of the ceramic window (see Fig. 1). This T-box structure also functions as a matching section between the power source and the coaxial transmission line module, enabling the high-power input coupler to maintain a low reflection coefficient. One end of the T-box connects to a standard 6-1/8" coaxial transmission line for input power, while the other end connects to the coaxial transmission line module of the coupler for output power. The third end serves as a short-circuit section, allowing adjustment of the power coupler's reflection coefficient and providing a cooling channel for the inner conductor of the ceramic window.

Based on the frequency of the RFQ cavity, a coaxial structure with a 50 Ω impedance was chosen for the coaxial transmission line module of the high-power input coupler.

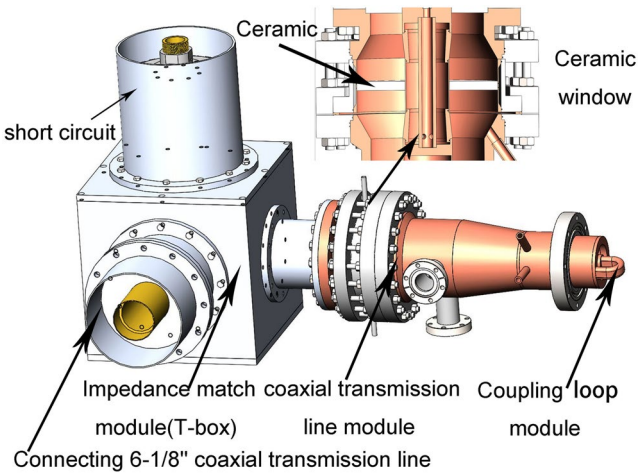

Fig. 1 (Color online) High-power input coupler structure schematic

The outer and inner conductor diameters connected to the cavity port were 81 mm and 24 mm, respectively. This module includes the coaxial line, ceramic window, and Teflon. The ceramic window divides the coaxial transmission line module into two parts. The first part connects to the coupling loop module, with its inner conductor linked to the ceramic window's inner conductor via a high-frequency inner bullet, and its outer conductor connected to the ceramic window using stainless steel flanges. The second part connects to a T-box at one end and to the ceramic window at the other, supported by Teflon polyethylene to sustain the outer conductor. To facilitate the replacement of only the RF window components in case of a ceramic window breakage, the ceramic window component connects to the outer conductor of the coaxial transmission line using knife-edge flanges.

The design of the RF window was based on the CiADS HWR010 162.5 MHz input power coupler [22], as depicted in Fig. 1. A coaxial disk-type ceramic, composed of 97.6 % Al_2O_3, served as the vacuum barrier. However, the introduction of ceramic windows led to impedance changes in the coaxial line, resulting in excessive power losses for the input power coupler. Thus, during the high-frequency design phase, optimization of the ceramic window components was necessary to minimize thermal stress and ensure excellent impedance matching. Variables optimized included the ceramic window's thickness, inner and outer diameters, and taper length. The ceramic's final thickness was 8 mm. Impedance matching was achieved by increasing the outer diameter and reducing the inner diameter of the ceramic window, resulting in an outer diameter of 128 mm. With the outer diameter of the cooling channel of the inner conductor less than 10 mm, a ceramic window with an inner diameter of 40 mm was chosen. To prevent multipactoring discharge on the surface, a 10 nm thickness TiN coating was applied to the ceramic window surface using sputtering technology [23–26]. A 10-nm thickness was selected for several reasons. Firstly, RF loss due to the TiN layer can be neglected at 162.5 MHz. Secondly, this thickness could be accurately measured for this dimension, ensuring uniformity of the ceramic window to within a few nanometers.

The performance targets of the CiADS RFQ coupler and those of other laboratories are summarized in Table 1 [21, 27, 28]. The structural schematic of the coupling loop is depicted in Fig. 1. The coupling loop is joined to the inner and outer conductors of the coaxial transmission line module via vacuum brazing, with an O-ring made of fluorine rubber used to seal the vacuum. The power loss of the coupling loop itself is inversely proportional to the diameter of the coupling loop conductor. Thus, the smaller the cross-sectional area of the coupling loop conductor, the higher the power loss of the coupling loop, resulting in greater thermal stress. Excessive thermal stress can alter the area of the coupling loop (coupling

Table 1 Design parameters of the RF input coupler for RFQ

Requirement	IFMIF	IMP	PKU	FNAL
Nominal frequency (MHz)	175	162.5	162.5	162.5
Duty cycle	100 %	100 %	100 %	100 %
Max. transmitted power (kW)	200	60	30	75
Nominal power (kW)	153	26	30	75
S11@ nominal frequency (dB)	–	−55.2	−62	−50
Line impedance (Ω)	50	50	–	50
Bandwidth@S11=−20 dB (MHz)	> 2	42	25	25

strength), thereby affecting its proper operation. Conversely, the larger the cross-section of the coupling loop conductor, the greater the volume of the coupling loop in the RFQ cavity, which can significantly alter the distribution of high-frequency electromagnetic fields within the cavity. Based on the analysis above, the parameters of the coupling loop are as follows: the length of the coupling loop inserted into the cavity was 32.5 mm, the cross-section of the coupling loop was 180 mm^2, the inner radius of the coupling loop was 14.5 mm, and the area of the coupling loop was 745 mm^2. Coupling strength, magnetic field strength around the loop, and surface loss density on the loop were evaluated using CST code. Considering that there may be three couplers when the RFQ cavity is in operation, the coupling strength was designed accordingly during the design stage. When the coupler is connected to the cavity, the mounting angle of the coupling loop can be adjusted to meet the demand for coupling strength of either four or three couplers. The coupling strength of the cavity is [29].

$$\beta = \frac{Q_0}{Q_{\text{ext}}} = \frac{P_{\text{ext}}}{P_{\text{cav}}} = \frac{(P_{\text{cav}} + P_{\text{beam}})}{P_{\text{cav}}} \tag{1}$$

The equivalent coupling strength of each coupling port is expressed as follows:

$$\beta_i^* = \frac{\beta_i}{1 + \sum_{i \neq j}^{4} \beta_j}. \tag{2}$$

The total coupling strength of the coupler is 1.11. When three couplers are used, the equivalent coupling strength of each coupler is 0.216, with an S11 of −3.75 dB. If four couplers are used, the equivalent coupling strength of each coupler is 0.1514, with an S11 of −2.65 dB.

In this coupler, there were three cooling channels: two for cooling the inner and outer conductors of the ceramic window and one for cooling the coupling loop. The water flow rate in all cooling channels was designed to be 1.6 m/s, with a pressure of 8 atm during the pressurization test.

3 Electromagnetic and structural design of the cavity

3.1 Design considerations for cavity

Due to the coupler's design power of 60 kW continuous wave, the following design criteria had been established to reduce cavity manufacturing costs and power losses:

(a) Compact structure and low costs. Large cavity dimensions impede transportation, low-temperature baking, and conditioning system assembly, while also increasing manufacturing costs. Therefore, a rigid coaxial transmission line with a diameter of 9-3/16" was used to process the inner and outer conductors of the cavity.
(b) High transmission efficiency and low power losses. High power losses in the cavity would elevate cooling requirements and gas exhaust, consequently prolonging test time and increasing costs.
(c) Tunable. Theoretical calculations show that the power loss rises from 4.6 % to 10 % (Fig. 5) as the cavity frequency deviates from the center frequency by 110 kHz. Cavity frequency shifts may occur due to cavity processing, gas pumping vibrations, and temperature increases. Thus, the cavity needs sufficient tuning capability to maintain low power losses during operation.
(d) Minimize K_p value and maximize coupling strength. If the RF electric field is sufficiently high, the room temperature copper cavity may experience RF electrical breakdown or sparking. The K_p value defines the maximum electric field achievable within the cavity without experiencing RF electrical breakdown or sparking at a given frequency. Hence, a smaller K_p value can decrease the likelihood of RF electrical breakdown or sparking.

The coupling strengths of the upstream and downstream couplers are β_1 and β_2, respectively. The power loss of the cavity (P_{cav}) [30] is as follows:

$$P_{\text{cav}} = \frac{4P_{\text{in}}\beta_1}{(1 + \beta_1 + \beta_2)^2}. \tag{3}$$

In Equation (3), P_{cav} represents cavity loss, and P_{in} represents the input power of the upstream coupler.

The dimensions of the coupling loops of the two couplers were determined before the tests. Thus, β_1 is equal to β_2. Then, the expression of P_{cav} is transformed into the following equation:

$$P_{\text{cav}} = \frac{4P_{\text{in}}\beta}{(1 + 2\beta)^2}. \tag{4}$$

The power extracted by the downstream coupler can be represented as $P_t = \beta_2 P_{cav}$. Substituting the value of Eq. (4) into this equation yields

$$P_t = \frac{4P_{in}\beta^2}{(1+2\beta)^2}. \quad (5)$$

Based on Eq. (4) and Eq. (5), cavity loss decreases and transmission power increases with higher coupling strength. A significant coupling strength suggests that the majority of the cavity's stored energy is efficiently transmitted to the external load via the power coupler, resulting in minimal cavity power loss. Thus, for cavities tasked with power transmission, a high coupling degree is desirable.

The high-power input coupler, supplying power to the superconducting cavity at a frequency of 166.6 MHz, utilized a QWR-type cavity for offline high-power conditioning [5]. Therefore, the quarter-wave resonator (QWR) cavity was chosen for the offline testing of the high-power coupler for the CiADS RFQ cavity, as depicted in Fig. 2. One side of the cavity, with a stronger magnetic field, was equipped with two ports for connecting the coupler, while the other side was also designed with two ports for connecting the tuner.

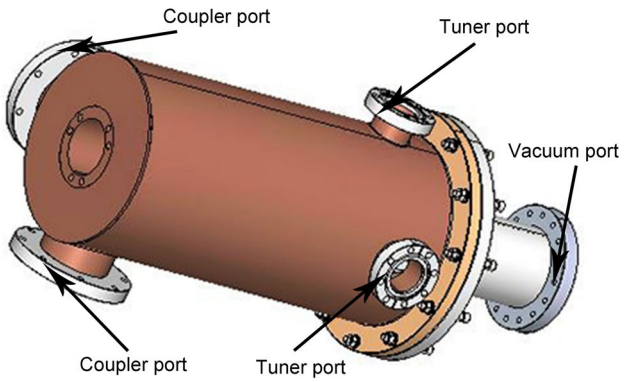

Fig. 2 (Color online) Cavity structure schematic

3.2 Electromagnetic design

The electromagnetic design and optimization of the offline test cavity were conducted using the three-dimensional electromagnetic simulation software CST. Since a rigid coaxial transmission line with a diameter of 9-3/16" was employed in manufacturing the cavity, the diameters of the inner and outer conductors were predetermined. The cavity's outer and inner conductor diameters were 240 mm and 100 mm, respectively. Consequently, the cavity's frequency could be adjusted to 162.5 MHz by altering the length of the inner conductor, as illustrated in Fig. 3a. From the figure, it is evident that increasing the length of the inner conductor leads to a decrease in frequency. This can be attributed to the increase in capacitance with length, resulting in a lower frequency. Beyond a length of 400 mm, the frequency decrease rate accelerates.

Figure 3b illustrates the cavity frequency as a function of the insertion depth of one of the tuners while the insertion depth of the other tuner remains constant. The tuning range of the tuner is 3.2 MHz. As depicted in the figure, increasing the insertion depth results in a lower frequency. However, excessive insertion depth reduces the gap between the inner conductor and the tuner, raising the maximum surface electric field of the cavity. This phenomenon increases the risk of RF electrical breakdown. To mitigate this, two tuners were designed. Upon cavity installation, the insertion depths of both tuners were adjusted to align the cavity frequency with the operating frequency. During operation, one tuner remains fixed while the other tuner's insertion depth is adjusted to maintain the cavity frequency around 162.5 MHz, thereby ensuring cavity losses remain within acceptable limits.

The position of the coupling loop during installation influences the coupling strength, which subsequently impacts S11 and cavity losses [31]. To assess how cavity and coupler processing errors, as well as mounting errors, affect cavity power losses, the effect of the coupling loop's rotation angle on the S-parameter was investigated. The results are depicted in Fig. 4. When the installation angle is 180°, as

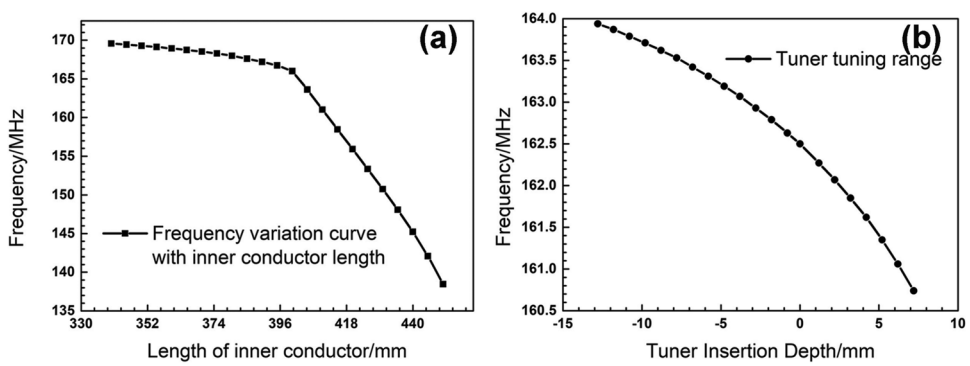

Fig. 3 **a** Variation of cavity frequency with the inner conductor; **b** variation of cavity frequency with tuner insertion depth

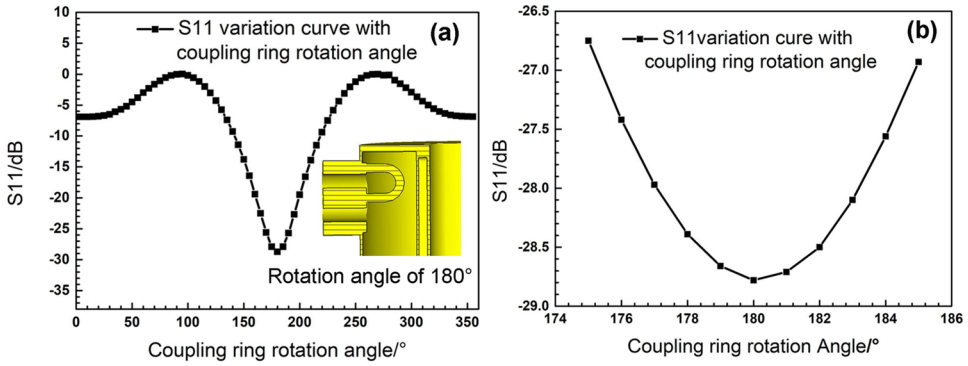

Fig. 4 Coupling ring rotation angle **a** 180°; **b** 180(5)°

shown in Fig. 4a, the magnetic flux within the area enclosed by the coupling loop is maximized, resulting in an S11 value of −28.77 dB. Using this angle as the reference point, S11 is maximized at a rotation of ±90°, minimizing the magnetic flux within the enclosed area of the coupling loop. Within the range of 180(5)°, S11 reaches its maximum, with a value of −2 dB (Fig. 4b). Therefore, adjusting the mounting angle of the coupling loop during assembly can minimize cavity power losses.

The final optimized *S*-parameters and electric field distribution are illustrated in Fig. 5. The simulated value of S21 for the cavity is −0.19 dB, corresponding to power losses of 4.3 %. In comparison, the power losses for the offline test cavities of the IFMIF and ESS RFQ cavity couplers are 7 % [20] and 4% [19], respectively. According to the conversion relationship between power losses and frequency [30], they equate to 7.26 % and 5.9 %, respectively. Therefore, the power losses of the offline test cavity for the CiADS RFQ cavity couplers are superior to the results reported in the literature. The simulated value of S11 for the test cavity is −28.77 dB, which closely aligns with values documented in the literature [19, 20] and can be considered acceptable. At an input power of 60 kW, the maximum electric field is 4.9 MV/m, the K_p value of the cavity is 0.42, and the coupling strength is 24.

3.3 Mechanical stability and thermal analysis

Due to the cavity's wall thickness being 5 mm, it is necessary to study the impact of temperature variation on its frequency. Thus, thermal and mechanical analysis of the cavity was conducted using the CST multiphysics module. In this study, the ambient temperature was set at 22 °C, and both the coupling loop and tuner, along with the inner conductor, were water-cooled at a flow rate of 1.6 m/s. A pressure of 0.1 MPa was applied to the cavity's outer wall. The results, depicted in Fig. 6, reveal that the cavity's maximum temperature, reaching 53.5 °C, occurs at the outer conductor due to its lack of cooling. The maximum stress within the cavity is 62 MPa, which is lower than the yield strength of oxygen-free copper [32]. The maximum displacement is 0.17 mm, resulting in a negligible change in frequency. These thermal and mechanical analysis findings confirm that the 5-mm wall thickness of the cavity meets the requirements for offline testing.

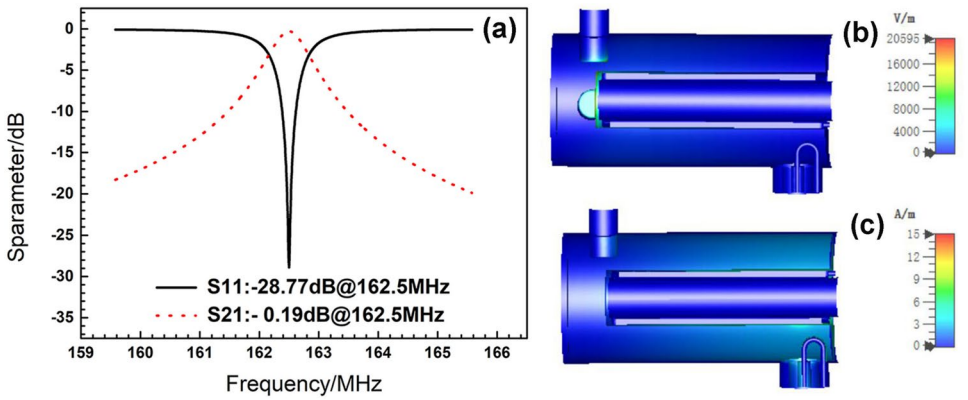

Fig. 5 (Color online) **a** S-parameter; **b** electric field distribution; **c** magnetic field distribution

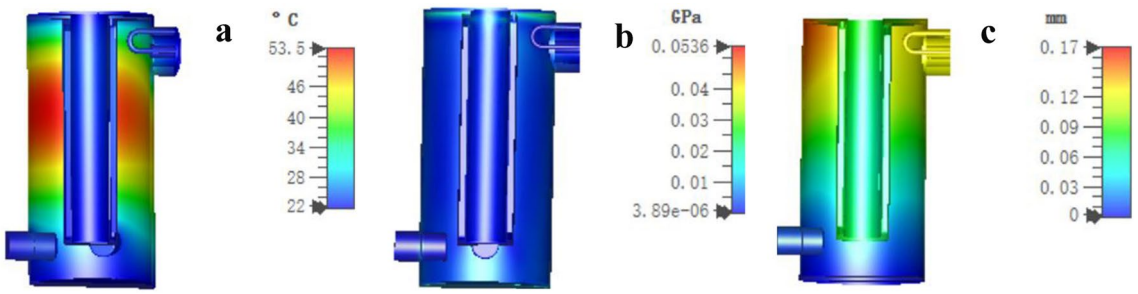

Fig. 6 (Color online) **a** Temperature distribution; **b** stress distribution; **c** displacement distribution

4 High-power offline test

4.1 Conditioning method

The CiADS RFQ high-power input coupler is designed for 60 kW power. However, due to the unavailability of a suitable power source at the Institute of Modern Physics, Chinese Academy of Sciences, we opted for standing wave resonance conditioning [33, 34], with a test power target of 20 kW. The drawback of this conditioning method is that it may not sufficiently condition the coupler due to the standing wave field. To address this, we adjusted the phase of the standing wave resonance conditioning system to maximize conditioning. Additionally, to enhance efficiency, we implemented the automatic sweeping amplitude method [31]. This method involves rapid scanning within a specific power range. Upon reaching the upper limit of high power, the vacuum is degassed, albeit briefly, allowing the vacuum pump adequate time to remove gas. This approach ensures that the vacuum remains superior to the conditioning system's threshold value and significantly distant from the protection threshold within a single scanning cycle. In the fixed point conditioning mode, the power remains constant, often resulting in the vacuum hovering near the threshold. When encountering severe vacuum outgassing at certain power points, vacuum protection may engage, or the power may automatically decrease per the logic of the automatic conditioning program, thus diminishing conditioning efficiency. Conditioning of power couplers begins with a low duty cycle and progresses to continuous wave, starting from low power and gradually increasing to high power. Initially, the conditioning process commences with a duty cycle of 1 % and a repetition frequency of 100 Hz. Subsequently, the duty cycle is incrementally raised to 5 %, 10 %, 30 %, 50 %, 80 %, and ultimately continuous wave operation.

4.2 Preparation conditions

Upon completion of cavity fabrication, the cavity underwent visual inspection, ultrasonic cleaning, drying with high-purity nitrogen gas, a 24-hour placement in a Class 100 cleanroom for drying, and vacuum leak detection. If the vacuum leak rate was better than 5×10^{-10} mbar L/s, the cavity was transported to the offline conditioning cleanroom and connected to two couplers as depicted in Fig. 7a.

The transmission characteristics of the entire offline conditioning system were tested using the R&S ZNB network analyzer from Rohde & Schwarz. The results are shown in Fig. 7b. To minimize power losses of the offline conditioning cavity during the test, the mounting angle of the rotating coupling loop was adjusted. The measured value of S21 for the entire conditioning system is −0.3 dB, corresponding to a loss of 6.3 %, compared to losses of 7 % [20] and 4 % [19] reported in the literature, respectively. Therefore, the power loss of the offline conditioning system in this paper is within an acceptable range. The simulated value of S21 for the cavity is −0.19 dB, corresponding to a loss of 4.3 %, as shown in Fig. 7b. The increase in measured power losses is attributed to the fact that the simulation was conducted under ideal conditions, without considering transmission line or coupler power losses. When the power loss of the conditioning system is 10 %, the frequency variation of the offline conditioning cavity is 132 kHz. During the test, we can adjust the frequency variation using the tuner to minimize power losses of the conditioning system.

After completing the transmission performance test of the offline conditioning system, it was vacuumed and baked at 120 °C (held for 48 h) to remove any residual moisture from the cleaning process. Subsequently, the high-power input couplers were installed on the offline conditioning platform, awaiting high-power conditioning, as depicted in Fig. 7c.

4.3 Offline conditioning

The high-power coupler offline conditioning system is depicted in Fig. 8. It comprises the coupler conditioning platform, power source system, low-level radio frequency, and peripheral auxiliary equipment. The conditioning platform features two couplers and a QWR cavity. The low-level radio frequency facilitates vacuum data acquisition,

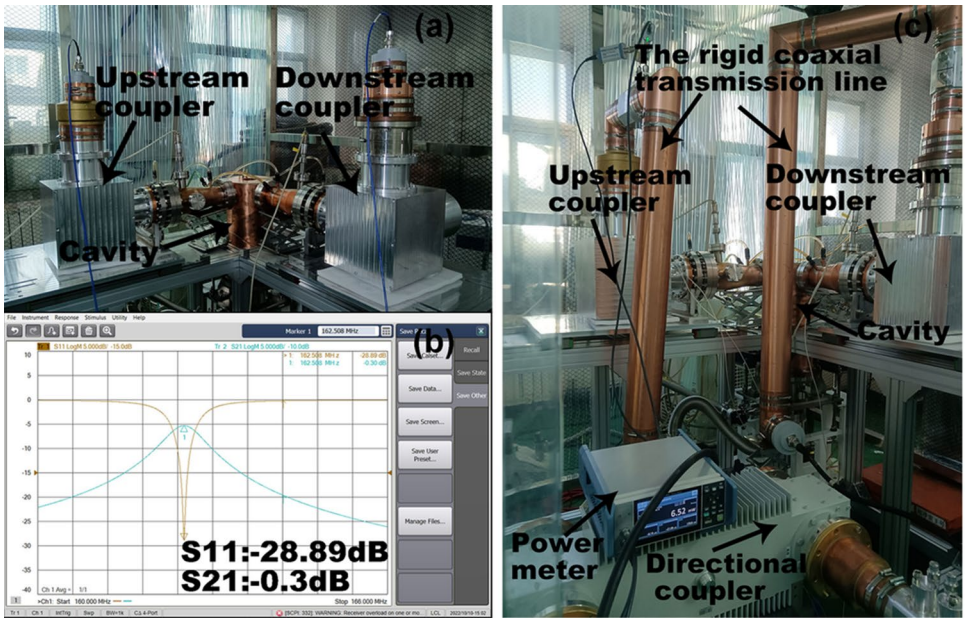

Fig. 7 (Color online) **a** *S*-parameter measurement diagram;**b** *S*-parameter measurement results; **c** offline conditioning platform

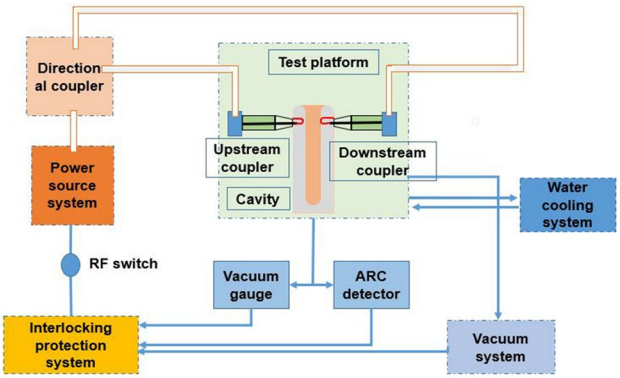

Fig. 8 High-power coupler offline conditioning system

ARC detection, implementation of conditioning mode, and safety interlock protection. The power source system encompasses a power source, signal source, directional coupler, and coaxial transmission lines. The power source is a 1 kW solid-state unit. Peripheral auxiliary components include a vacuum pump system and water chiller. Power output from the source enters the directional coupler and then passes through the upstream coupler, conditioning cavity, downstream coupler, and another directional coupler. This cycle continues multiple times. The entire conditioning system forms a resonant system, with the system frequency adjusted to 162.5 MHz by altering the length of the coaxial transmission line.

Due to the coupler being more likely to outgas under low-power conditions, the traveling wave conditioning mode was employed at power levels below 1 kW. In this mode, the downstream coupler was connected to a matched load. When the solid-state power source exceeded its power limit, the standing wave resonance conditioning system was used for the test. After processing the power coupler and conditioning cavity, there are usually burrs, dust, and small metal particles on their inner surfaces. Therefore, at the beginning of conditioning, outgassing is typically severe. Generally, a pulse conditioning mode was used, with the duty cycle gradually increasing from 1 to 100 %. Real-time monitoring of the coupler and cavity vacuum, as well as coupler ARC discharge, was carried out during conditioning. The vacuum protection threshold was set to 5×10^{-4} mbar L/s. After 60 h of conditioning, the standing wave power reached 26.5 kW in continuous wave mode. The maximum temperature for the upstream and downstream coupler on the T-box inner conductor was 55.1 °C and 47.5 °C, respectively. The maximum temperature of the outer conductor of the cavity was 42.9 °C, and the inner conductor temperature was 22.1 °C (Fig. 9).

To adequately condition the power coupler, the standing wave point of the power coupler was adjusted by modifying the phases of the entire standing wave resonance conditioning system. During the conditioning process, the phase difference between the two standing wave points of the conditioning system is 15°. Upon completion of the conditioning, the vacuum and power change curves during the loading process from zero power to the target power are depicted in Fig. 10. The phase of the standing wave resonance conditioning system was set at 180°, with a duration of 1 h. From this figure, it is evident that the maximum standing wave power is 25 kW in continuous wave mode, which exceeds the target power.

Fig. 9 (Color online) Conditioning result: **a** power; **b** temperature distribution

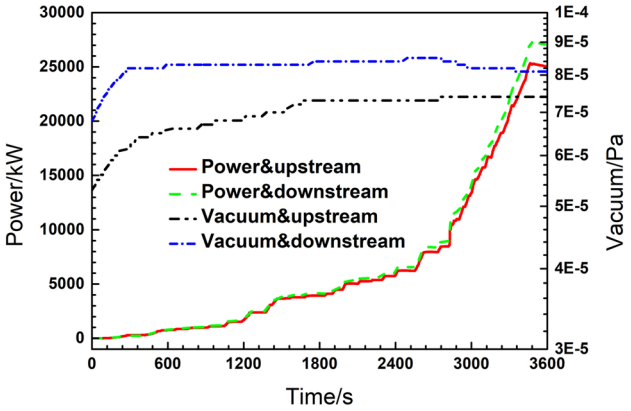

Fig. 10 High-power conditioning results at a phase angle of 180°

5 Conclusion

To verify the rationality of the design of the power coupler for the CiADS RFQ cavity and reduce cavity contamination, this study designed a low-loss offline conditioning cavity and conducted a high-power test. The conclusions are as follows:

The conditioning cavity utilized a QWR-type cavity, featuring two coupling ports and two tuners. Minimizing cavity loss was achieved through adjusting the installation angle of the coupling loop and the insertion depth of the tuner. Electromagnetic structural and multiphysics simulations of the cavity were conducted using 3D microwave simulation software CST. The transmission efficiency was studied by varying tuner insertion depth, inner conductor length, and coupling strength. The optimal theoretical power loss was 4.3 %, outperforming the reported literature values. At a frequency variation of 110 kHz, the theoretical power loss increased to 10 %, necessitating continuous tuner adjustment during conditioning. With a coupling strength of 24, the cavity exhibited minimal power loss, indicating efficient power transfer through the coupling loop. Multiphysics simulations demonstrated that cavity temperature variations did not affect frequency. Upon completion of the offline high-power conditioning platform, the transmission performance of the entire system was measured, yielding a power loss of 6.3 %, slightly higher than the theoretical calculation. This discrepancy may be attributed to processing, material properties, and transmission line effects, which were not accounted for in the theoretical model. Conditioning utilized efficient automatic range scanning and standing wave resonant methods. Traveling wave mode was employed for conditioning under 1 kW to address vacuum outgassing. Adjusting the phase difference between two standing wave points by 15° ensured thorough conditioning of the power coupler. The maximum continuous wave power exceeded 20 kW, surpassing the target, thereby ensuring stable operation of the CiADS RFQ accelerator cavity.

Author contributions All authors contributed to the study conception and design. Material preparation and data collection and analysis were performed by Ruo-Xu Wang, Yuan He, Long-Bo Shi, Chen-Xing Li, Zong-Heng Xue, Tian-Cai Jiang, Xian-Bo Xu, Lie-Peng Sun, and Zhou-Li Zhang. The first draft of the manuscript was written by Ruo-Xu Wang and Zhou-Li Zhang, and all authors commented on previous versions of the manuscript. All authors read and approved the final manuscript.

Data availibility The data that support the findings of this study are openly available in Science Data Bank at https://doi.org/10.57760/sciencedb.j00186.00133 and https://cstr.cn/31253.11.sciencedb.j00186.00133

Declarations

Conflict of interest The authors declare that they have no Conflict of interest.

References

1. S.H. Liu, Z.J. Wang, H. Jia et al., Physics design of the CIADS 25 MeV demo facility. Nucl. Instrum. Meth. A **843**, 11 (2017). https://doi.org/10.1016/j.nima.2016.10.055

2. Y.L. Huang, L.B. Liu, T.C. Jiang et al., 650 MHz elliptical superconducting RF cavities for CiADS project. Nucl. Instrum. Meth. A **988**, 164906 (2021). https://doi.org/10.1016/j.nima.2020.164906
3. W.L. Chen, Z.J. Wang, S.H. Liu et al., Physics design of the CiADS MEBT. Int. J. Mod. Phys. A **36**, 2150127 (2021). https://doi.org/10.1142/S0217751X2150127X
4. Y.Q. Liu, D.H. Zhuang, F. Wang et al., The performance of RF power couplers with capacitive coupling for SRF accelerators. Nucl. Instrum. Meth. A **1010**, 165565 (2021). https://doi.org/10.1016/j.nima.2021.165565
5. T.M. Huang, P. Zhang, Q. Ma et al., Development of fundamental power couplers for 166.6 MHz superconducting quarter-wave beta= 1 proof-of-principle cavities. Rev. Sci. Instrum. **91**, 063301 (2020). https://doi.org/10.1063/5.0001540
6. S. Michizono, Secondary electron emission from alumina RF windows. IEEE Trans. Dielect Electr. Insul. **14**, 3 (2007). https://doi.org/10.1088/1674-1137/37/2/024102
7. F. Lin, Y. Ding, B. Shen et al., Research on cylindrical box type windows used to transmit high power CW. J. Electron. **21**, 392 (2004). https://doi.org/10.1007/BF02687940
8. P. Ylae-Oijala, M. Ukkola, Suppressing electron multipacting in ceramic windows by DC bias. Nucl. Instrum. Meth. A **474**, 197 (2001). https://doi.org/10.1016/S0168-9002(01)00882-8
9. R.L. Geng, H. Padamsee, S. Belomestnykh et al., Suppression of multipacting in rectangular coupler waveguides. Nucl. Instrum. Meth. A **508**, 3 (2003). https://doi.org/10.1016/S0168-9002(03)01660-7
10. H.P. Ouyang, J.M. Qiao, S.N. Fu et al.,Physical design study on the input coupling loop of radio frequency quadrupole with intense beams. High Power Laser and Particle Beams **16**, 117 (2004). (**in Chinese**) https://www.hplpb.com.cn/article/id/668
11. L. Chen, Dissertation, Development of a room-temperature test system for high power input coupler. University of Chinese Academy of Sciences (2018). (**in Chinese**)
12. E. Chojnackie, S. Belomestnykh, RF power coupler performance at CESR and study of a multipactor inhibited coupler. In: *Proceedings of the 1999 Workshop on RF Superconductivity*, Los Alamos, New Mexico, 1–5 November (1999)
13. B. Dwersteg, D. Kostin, M. Lalayan et al., Tesla RF power couplers development at DESY. In: *Proceedings of the 10th Workshop on RF Superconductivity*, Tsukuba, Ibaraki, 6–11 September (2001)
14. C.W. Ma, X.M. Bao, J. Yu et al., Neutron density distributions of neutron-rich nuclei studied with the isobaric yield ratio difference. Eur. Phys. J. A **50**, 139 (2014). https://doi.org/10.1140/epja/i2014-14139-1
15. M. Stirbet, G.K. Campisi, G.K. Davis et al., Processing test stand for the fundamental power couplers of the Spallation Neutron Source (SNS) superconducting cavities, In: *Proceedings of the 2001 Particle Accelerator Conference*, Chicago, Illinois, 18–22 (June 2001)
16. E.N. Schmierer, C.D. Chan, D.C. Gautier et al., High-power testing of the APT power coupler. In: *Proceedings of the 10th Workshop on RF Superconductivity*, Tsukuba, Ibaraki, 6–11 (September 2001)
17. E. Montesinos, Construction and processing of the variable RF power couplers for the LHC superconducting cavities. In: *Proceedings of the 13th Workshop on RF Superconductivity*, Peking University, Beijing,11–19 (October 2007)
18. X. Chen, F.B. Meng, Q. Ma et al., Coupler conditioning and high power testing of ADS Spoke cavity. Chin. Phys. C **38**, 027001 (2014). https://doi.org/10.1088/1674-1137/38/2/027001
19. N. Misiara, A.C. Chauveau, D. Chirpaz-Cerbat et al., The saclay test stand for conditioning the ess rfq power coupler at high power. In: *Proceedings of the 9th International Particle Accelerator Conference*, University of British Columbia, Vancouver, BC, Canada 29 April, 2018. pp. 2375–2377. https://doi.org/10.18429/JACoW-IPAC2018-WEPMF004
20. E. Fagottie, L. Antoniazzi, M. Giacchini et al., The couplers fot the IFMIF-EVEDA RFQ high power test stand at LNAL design, construcion and operation, In: *Proceedings of the 27th International Linear Accelerator Conference*, Geneva, Canton of Geneva, 31 August (2014). pp. 643–645. https://accelconf.web.cern.ch/LINAC2014/papers/tupp093.pdf
21. S. Maebara, A. Palmieri, P. Mereu et al., Engineering design of the RF input coupler for the IFMIF prototype RFQ linac. Fusion. Eng. Des. **88**, 2740 (2013). https://doi.org/10.1016/j.fusengdes.2013.02.135
22. T.C. Jiang, Development of a dual warm windows power coupler. Dissertation, University of Chinese Academy of Sciences (2019). (**in Chinese**)
23. Z. Lu, S. Fukuda, Z. Zhou et al., Design and development of radio frequency output window for circular electron-positron collider klystron. Chin. Phys. B **27**, 11 (2018). https://doi.org/10.1088/1674-1056/27/11/118402
24. Y. Ding, *Design, Manufacture and application of high power klystron*, 1st edn. (National Defense Industry Press, Arlington, 2010), pp.269–271
25. Z. Peng, G. Chen, Y. Zhao et al., Investigation of TiN film on an RF ceramic window by atomic layer deposition. J. Vac. Sci. Technol. A **38**, 052401 (2020). https://doi.org/10.1116/6.0000159
26. S.C. Wang, Z.S. Zhou, Z.J. Lu et al., Development of RF windows for 650 MHz multibeam klystron. Nucl. Sci. Tech. **34**, 136 (2023). https://doi.org/10.1007/s41365-023-01294-0
27. Q. Fu, K. Zhu, Y.R. Lu et al., Design and cold model experiment of a continuous-wave deuteron radio-frequency quadrupole. Nucl. Instrum. Meth. A **20**, 120101 (2017). https://doi.org/10.1103/PhysRevAccelBeams.20.120101
28. S. Kazakov, O. Pronitchev, V. Poloubotko et al., Design of 162.5 MHz CW main coupler for RFQ, In: *Proceedings of the 27th International Linear Accelerator Conference*, Geneva,Canton of Geneva, 31 August-5 September (2014)
29. C.X. Li, Y. He, F.F. Wang et al., Radio frequency measurements and tuning of the China material irradiation facility RFQ. Nucl. Instrum. Meth. A **890**, 43 (2018). https://doi.org/10.1016/j.nima.2018.02.047
30. T.P. Wangler, *RF Linear Accelerators*, 2nd edn. (Wiley-VCH, Weinheim City, 2008), p.145
31. L. Chen, S.H. Zhang, Y.M. Li et al., Room-temperature test system for 162.5 MHz high-power couplers. Nucl. Sci. Tech. **30**, 7 (2019). https://doi.org/10.1007/s41365-018-0531-9
32. Z.L. Zhang, X.B. Xu, Y. He et al., Design of a radio frequency quadrupole for a high intensity heavy-ion accelerator facility. Phys. Rev. Accel. Beams. **25**, 080120 (2022). https://doi.org/10.1103/PhysRevAccelBeams.25.080102
33. S. Kazakov, B. Hanna, O. Pronitchev, Testing of 325MHZ couplers at test stand in resonance mode. In: *Proceedings of the 2015 Workshop on RF Superconductivity*, University of British Columbia, Vancouver, 13–18 (September 2015)
34. S. Maebara, M. Sugimoto, RF properties of A 175 MHz high Q load circuit. In: *Proceedings of 8th International Particle Accelerator Conference*, Copenhagen, Denmark, 14–19 (May 2017)